Simultaneous SU(2) rotations on multiple quantum dot exciton qubits using a single shaped pulse

Reuble Mathew, Hong Yi Shi Yang, and Kimberley C. Hall
Department of Physics and Atmospheric Science, Dalhousie University, Halifax, Nova Scotia B3H4R2, Canada
(Received 25 June 2015; revised manuscript received 28 August 2015; published 8 October 2015)

Recent experimental demonstration of a parallel (π, 2π) single qubit rotation on excitons in two distant quantum dots [Nano Lett. **13**, 4666 (2013)] is extended in numerical simulations to the design of pulses for more general quantum state control, demonstrating the feasibility of full SU(2) rotations of each exciton qubit. Our results show that simultaneous high-fidelity quantum control is achievable within the experimentally accessible parameter space for commercial Fourier-domain pulse shaping systems. The identification of a threshold of distinguishability for the two quantum dots (QDs) for achieving high-fidelity parallel rotations, corresponding to a difference in transition energies of $\sim$0.25 meV, points to the possibility of controlling more than 10 QDs with a single shaped optical pulse.

DOI: 10.1103/PhysRevB.92.155306 PACS number(s): 78.67.Hc, 78.55.Cr, 71.38.−k, 78.47.J−

I. INTRODUCTION

Optimal quantum control (OQC) describes the science of controlling the evolution of quantum systems to transfer an initial state to a desired final state [1,2]. (For a recent review, see Ref. [3].) In quantum systems controlled by laser fields, one can use sophisticated pulse-shaping techniques coupled with closed-loop evolutionary algorithms to manipulate the interaction Hamiltonian that governs the dynamics. Adaptive algorithms are particularly effective for the optimization of imprecisely characterized systems [4,5] or for those with a numerically intractable system Hamiltonian. They have, for example, been used to control chemical reaction pathways [6,7], to detect molecular species [8], and to generate high harmonics [9,10]. In the field of quantum information science, OQC may be applied to the optimization of quantum gate fidelity and/or operating speed. This approach has been applied in recent experiments involving multiple-qubit gates in trapped ion systems [11] and superconducting qubits [5], as well as spin entanglement in nitrogen vacancies [12]. OQC could also aid in the development of complex instruction set approaches to quantum computing, wherein multiple single- and two-qubit gates are replaced with a single system transformation, reducing the time required to carry out the computation while exploiting the relative ease of control pulse engineering [13]. Progress along these lines has been realized in molecular qubit systems with the demonstration of a multiple-input AND gate [14]. The achievement of such goals in scalable solid state systems is particularly attractive due to the advantages of such platforms in terms of future integration with classical technologies.

Among the solid state systems being explored for quantum-enabled device development, semiconductor quantum dots (QDs) offer a number of advantages. A QD-based device architecture would leverage existing semiconductor and photonic fabrication infrastructure with the possibility of optically mediated quantum state control and read-out at telecommunication wavelengths, facilitating integration with existing hardware. The implementation of short laser pulses for rapid manipulation of QD excitations paves the way toward fast quantum gates and potential THz operation rates. Demonstrations of fundamental quantum control processes involving charge and spin states in QDs have included single-qubit rotations (involving excitons [15–19], biexcitons [20,21], and single carrier spins [22,23]), quantum state tomography [18,24–29], manipulation of exciton spin superpositions [30,31], the establishment of entanglement between excitons [32–34], and the use of an optical microcavity for selective control of QDs within an ensemble [35]. These studies illustrate the ease of coherent optical control of quantum states within semiconductor QDs; however, the exclusive use of control pulses with constant phase severely limits the scope and flexibility of the quantum control process.

The extension of the above optical control experiments to tailored quantum state control via OQC in QDs has been explored in recent years [36–38]. A reduction in the control pulse duration for a C-ROT gate involving two exciton qubits confined to a single QD [32,39] to the subpicosecond regime was demonstrated in numerical applications of OQC [36,38], where pulse shaping ensured the achievement of high-fidelity conditional dynamics despite the large pulse bandwidth. General pulse shape engineering has also been applied experimentally in the implementation of simultaneous π and 2π single qubit rotations in two uncoupled QDs using a single laser pulse [37]. These proof-of-principle experiments demonstrated the feasibility of parallel quantum computing enabled by the stochastic variations in optoelectronic properties that result from the quantum dot self-assembly process. In this work, we numerically explore the ability to achieve independent SU(2) control of excitons in a pair of quantum dots using a single shaped pulse. Our calculations show that high fidelity parallel qubit rotations can be found for an arbitrary choice of state inversions and phases of the two exciton qubits provided the pair of QDs utilized have sufficiently different optoelectronic properties: A difference in *either* the dipole moment ($\sim$2 debye) *or* transition energy ($>$0.25 meV) is sufficient, commensurate with typical variations in self-assembled quantum dot ensembles [19,40–43]. These findings demonstrate the feasibility of parallel quantum state control in systems of more than 10 quantum dots using conventional laser and pulse shaping systems. The simultaneous manipulation of multiple qubits using a single shaped laser pulse would help reduce the required laser resources for qubit control and promote scalability of these systems for quantum information processing.

II. OPTIMAL QUANTUM CONTROL: NUMERICAL METHODS

We model each QD as a two-level system, defined by states $|0\rangle$ and $|1\rangle$ that are separated in energy by $\hbar\omega_{10}$. The qubits possess an optical dipole moment $\boldsymbol{\mu}_{10} = \langle 1|\boldsymbol{\mu}|0\rangle$, which allows for manipulation using an ultrafast laser pulse with an electric field given by

$$\mathbf{E}(t) = \tfrac{1}{2}\hat{\boldsymbol{\epsilon}} E_0(t)\{e^{-i[\omega_l t+\phi]} + e^{+i[\omega_l t+\phi]}\}. \tag{1}$$

Here $\hat{\boldsymbol{\epsilon}}$ is a unit vector representing the polarization state of the laser field, $E_0(t)$ is the field envelope, ω_l is the center frequency of the laser pulse, and ϕ is the pulse phase. The control Hamiltonian for the two-level system in the presence of the light field is given in the rotating wave approximation (RWA) by

$$H = \frac{\mathrm{Re}[\hbar\Omega_R]}{2}\hat{\sigma}_x + \frac{\mathrm{Im}[\hbar\Omega_R]}{2}\hat{\sigma}_y + \frac{\hbar\Delta}{2}\hat{\sigma}_z, \tag{2}$$

where $\hbar\Omega_R = (\boldsymbol{\mu}_{10}\cdot\hat{\boldsymbol{\epsilon}})\, E_0(t)e^{-i\phi}$ is the complex Rabi energy, $\Delta = \omega_{10} - \omega_l$ is the detuning of the laser from the QD transition, and $\hat{\sigma}_{x,y,z}$ are the Pauli spin matrices. The resulting equation of motion for the Bloch vector $\mathbf{s}$, where $s_j = \langle\hat{\sigma}_j\rangle$, is

$$\dot{\mathbf{s}} = \mathbf{s}\times\boldsymbol{\Lambda}, \tag{3}$$

which describes the rotation of the Bloch vector about a torque vector $\boldsymbol{\Lambda} = (-\mathrm{Re}[\Omega_R], -\mathrm{Im}[\Omega_R], \Delta)$ determined by the characteristics of the optical pulse.

During a Rabi rotation, for which $\Delta = 0$ and ϕ is constant in time, the direction of $\boldsymbol{\Lambda}$ does not change during the control pulse and the Bloch vector rotates about a fixed axis. Shaping the laser pulse [e.g., by incorporating a time-dependent phase $\phi(t)$] leads to a time-dependent control vector $\boldsymbol{\Lambda}$, thereby allowing for deterministic control over the trajectory of the Bloch vector and/or the choice of target final quantum state. We demonstrate the versatility of this approach to coherent control of multiple solid state qubits by applying general pulse engineering to the optimization of simultaneous single qubit rotations for excitons confined to two uncoupled quantum dots, referred to as QD1 and QD2. This approach was used in Ref. [37] to implement simultaneous $(\pi, 2\pi)$ rotations, representing an experimental demonstration of independently specified occupation states. Here we extend this to the design of numerically optimized pulses for arbitrary SU(2) control of the two quantum dot excitons. We note that, in real QDs for the most typical case of growth on [001]-oriented substrates, the anisotropic exchange interaction and elongation of the quantum dots with their long (short) axes aligned along [110] ($[1\bar{1}0]$) leads to two exciton transitions with orthogonally-polarized dipole moments, forming a V-system involving the crystal ground state [44–46]. While it may be possible to exploit the polarization state of the light field to enhance the degree of flexibility of the optimal quantum control process [46], our treatment of the exciton system in each QD as a simple two-level system reflects our choice here to restrict the controlling light field to linearly polarized pulses aligned with one of the symmetry directions of the quantum dots, together with the slow carrier spin relaxation in these systems [44].

In the general case, the amplitude, phase, and frequency of the control laser pulse can be manipulated in either the time domain by using devices such as acousto-optic modulators or in the frequency domain by placing controllable elements in the Fourier plane of a $4f$ pulse shaper. The most common approach for frequency-domain shaping, for which the optimum pulse shapes obtained here are intended, is to use a programmable liquid crystal spatial light modulator (SLM) containing an array of nematic liquid crystal elements each with an electrically tunable index of refraction [47]. The effect of the SLM in the Fourier plane on the laser pulse can be described by a mask function $M(\omega)$ that alters the input pulse spectrum $\tilde{E}_{\mathrm{in}}(\omega)$ to produce an output spectrum, $\tilde{E}_{\mathrm{out}}(\omega)$, given by

$$\tilde{E}_{\mathrm{out}}(\omega) = M(\omega)\tilde{E}_{\mathrm{in}}(\omega). \tag{4}$$

The input pulse spectrum $\tilde{E}_{\mathrm{in}}(\omega)$ is the Fourier transform of a Gaussian pulse with constant phase ϕ and a field envelope $E_0(t) = |E_0|\exp[-2\ln(2)t^2/\tau^2]$, with $\tau = 120$ fs. A dual-mask SLM can provide independent control over the amplitude and phase of the frequency components, such that the mask function can be defined in terms of an amplitude mask $A_M(\omega)$ and phase mask $\phi_M(\omega)$, where

$$M(\omega) = A_M(\omega)\exp[i\phi_M(\omega)]. \tag{5}$$

The desired form of $A_M(\omega)$ and $\phi_M(\omega)$ can be determined using numerical techniques that optimize any desired attribute of the quantum control process. In this work, we apply OQC to optimize the fidelity of parallel single qubit rotations involving multiple uncoupled semiconductor QDs.

We apply a phase-only mask [$A_M(\omega) = 1$], which has the advantage of reducing light losses in the system [36]. Any convenient function may be used to parametrize $\phi_M(\omega)$. Here we adopt a sinusoidal phase mask, given by

$$\phi_M(\omega) = \alpha\cos[\gamma(\omega-\omega_l) - \delta]. \tag{6}$$

The parameters α, γ, δ, and the pulse area $\Theta = (\boldsymbol{\mu}\cdot\hat{\boldsymbol{\epsilon}}/\hbar)\int_{-\infty}^{+\infty} E_0(t)\,dt$ are optimized numerically subject to the following constraints:

$$\begin{aligned} 0 &\leqslant \alpha \leqslant \pi, \\ 0 &\leqslant \gamma \leqslant 325\ \mathrm{fs}, \\ -\pi &\leqslant \delta \leqslant \pi, \\ 0 &\leqslant \Theta \leqslant 8\pi. \end{aligned} \tag{7}$$

The limits on α and γ are chosen to restrict the gradient in the phase $|d\phi_M(\omega)/d\omega|_{\max}$ to $\pi/10$ radians per pixel assuming the resulting optimized pulses are implemented on a pulse shaping system containing a 128 pixel SLM. This is a conservative requirement as commercial pulse shapers with a pixel count of 640 are readily available. (The implications of the resolution of the phase mask are discussed in more detail below.) The constraints on Θ are intended to simplify the experimental implementation, although Rabi rotations of up to 14π have been achieved in similar QDs [48].

For a given choice of the parameters in Eq. (6), the fidelity of the operation is defined as $F = \mathrm{Tr}[\rho_{\mathrm{P}}\rho_{\mathrm{I}}] = f(\alpha,\gamma,\delta,\Theta)$, where ρ_{P} is the physical density matrix at the end of the control process, calculated by integrating Eq. (3), and ρ_{I} is the ideal density matrix for the intended parallel single qubit rotation. We search for local optima in fidelity

$F_{\rm opt} = f(\alpha_{\rm opt},\gamma_{\rm opt},\delta_{\rm opt},\Theta_{\rm opt})$ by choosing initial vectors containing the free parameters α, γ, δ, and Θ, denoted by $q_i = (\alpha_i,\gamma_i,\delta_i,\Theta_i)$, and using the constrained optimization by linear approximations algorithm. We choose 500 initial vectors using a Sobol' sequence [49] to provide sufficient coverage of the four-dimensional space defined by Eq. (7). The parameters corresponding to local optima with the highest fidelity determine the optimal pulse shape. In the RWA, the phase of the qubit oscillates at a frequency Δ even after the end of the pulse. Therefore, we determine the fidelity of the control process by reading the state of the qubits at a fixed time $t = 3$ ps after the arrival of the laser pulse [$t = 0$ in Eq. (1)]. In experimental implementations of quantum algorithms, flexibility in the timing of multiple control pulses would likely be exploited. The stringent requirement of a fixed read time allows us to explore the quality of arbitrary final state control under the most conservative conditions.

III. RESULTS AND DISCUSSION

A. Arbitrary rotations of QD excitons

Figure 1 presents exemplary results of parallel control of excitons in two different QDs. For all results in this work, the laser pulse has a fixed tuning with $\hbar\omega_l = 1.0$ eV. For the calculation in Fig. 1, the transition energies of the two QDs are $\hbar\omega_{\rm QD1} = 1.00125$ eV and $\hbar\omega_{\rm QD2} = 0.99875$ eV, chosen to be within the bandwidth of the controlling laser pulses, and the dipole moments are taken as $\mu_{\rm QD1} = 25$ debye and $\mu_{\rm QD2} = 28$ debye, reflecting typical values for self-assembled QDs [19]. For these results, the pulse is optimized assuming

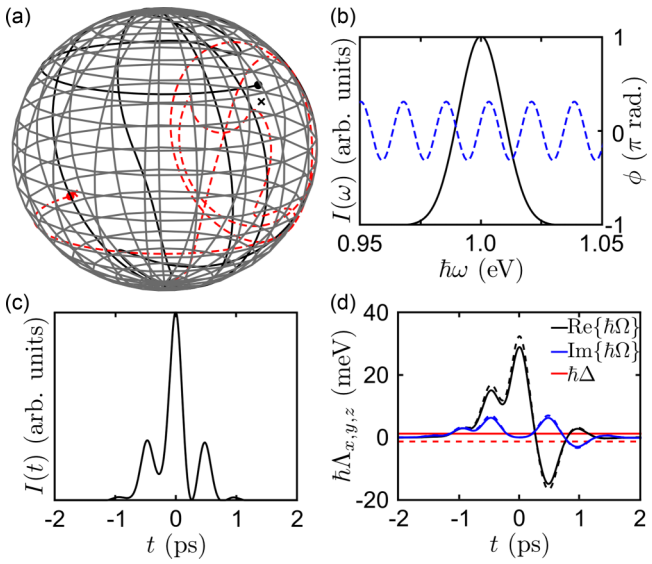

FIG. 1. (Color online) Application of OQC to quantum control transferring the excitons in QD1 and QD2 from their respective ground states to the final states in Eq. (8). (a) Bloch sphere dynamics for QD1 (QD2) are indicated by a black solid (red dashed) curve. (b) The spectral amplitude (phase) of the pulse are indicated by a black solid (blue dashed) curve. (c) Temporal intensity of the shaped pulse. (d) The x, y, and z components of $\mathbf{\Lambda}$ are indicated by black, blue, and red curves, respectively, with solid curves corresponding to QD1 and the dashed curves corresponding to QD2.

that the qubits are initialized in their respective ground states ($|\psi_{\rm QD1}\rangle_{\rm i} = |0\rangle$, $|\psi_{\rm QD2}\rangle_{\rm i} = |0\rangle$) with a target set of final states for the two QDs given by

$$|\psi_{\rm QD1}\rangle_{\rm f} = \tfrac{1}{2}(|0\rangle + e^{-i\pi/2}\sqrt{3}|1\rangle), \quad \text{and}$$
$$|\psi_{\rm QD2}\rangle_{\rm f} = \tfrac{1}{2}(\sqrt{3}|0\rangle + e^{-i3\pi/2}|1\rangle). \tag{8}$$

The final quantum states in Eq. (8) contain different state inversions and phases for the two QDs, providing a useful test to illustrate the OQC approach. Figure 1(a) shows the trajectory of the Bloch vector of QD1 (QD2) when driven by the optimized laser field, represented by the black solid (red dashed) curves, with the final quantum state of the two-dot system at the chosen read time of 3 ps indicated by the black (red) dot. The target final states in Eq. (8) for QD1 (QD2) are indicated on the Bloch sphere by a black (red) cross. The optimal pulse, characterized by parameters $q_{\rm opt} = (0.312\pi, 235\ {\rm fs}, 0.373\pi, 3.25\pi)$, implements the simultaneous qubit rotation with a fidelity of 0.996. This high fidelity is evident on the Bloch spheres by the close proximity of the final states for each QD and the respective target final states. Figure 1(b) shows the spectral intensity (black solid curve) and phase (blue dashed curve) of the corresponding optimal pulse, and Fig. 1(c) shows the resulting temporal field intensity. The temporal evolution of the three components of the optical torque vector, $\mathbf{\Lambda}$, that drives the qubit dynamics of QD1 (QD2) is shown in Fig. 1(d) as solid (dashed) curves. The high-fidelity control process depicted in Fig. 1(a), with a target final state that differs for the two quantum dots in both inversion and phase, illustrates the efficacy of pulse shape control for independently tailoring the quantum state dynamics of the excitons in the two quantum dots.

We explore the flexibility of this scheme for achieving a range of final states by optimizing the fidelity as a function of the difference in inversion, denoted by $\delta s_z = s_{z,\rm QD2} - s_{z,\rm QD1}$, taking $s_{z,\rm QD2} = -s_{z,\rm QD1}$, and the difference in phase of the two qubits, denoted by $\delta\phi = \phi_{\rm QD2} - \phi_{\rm QD1}$, taking $\phi_{\rm QD2} = -\phi_{\rm QD1}$. The resulting final state space spans all representative states on the Bloch spheres for the two QDs. The input laser characteristics, QD initial states, transition frequencies, and dipole moments are identical to those used for the calculated results in Fig. 1. The featureless contour plot in Fig. 2(a) demonstrates that optimized pulses producing high fidelity can be found for any choice of δs_z and $\delta\phi$ within the defined parameter space of Eq. (7). This result indicates that arbitrary independent high-fidelity control of the two quantum dot excitons is feasible using the OQC approach and general pulse shape engineering.

B. Dependence on QD optoelectronic properties

Next we implement optimal quantum control involving the target final quantum states in Eq. (8) and allow the optoelectronic properties of QD2 to vary while holding the properties of QD1 constant. The results of these calculations are presented in Fig. 2(b). If the QDs have nearly identical optoelectronic properties, it is impossible to find any pulse shape that drives the qubits from the same initial state to two different final states with high fidelity, leading to the dip in fidelity in Fig. 2(b) where the properties of QD1

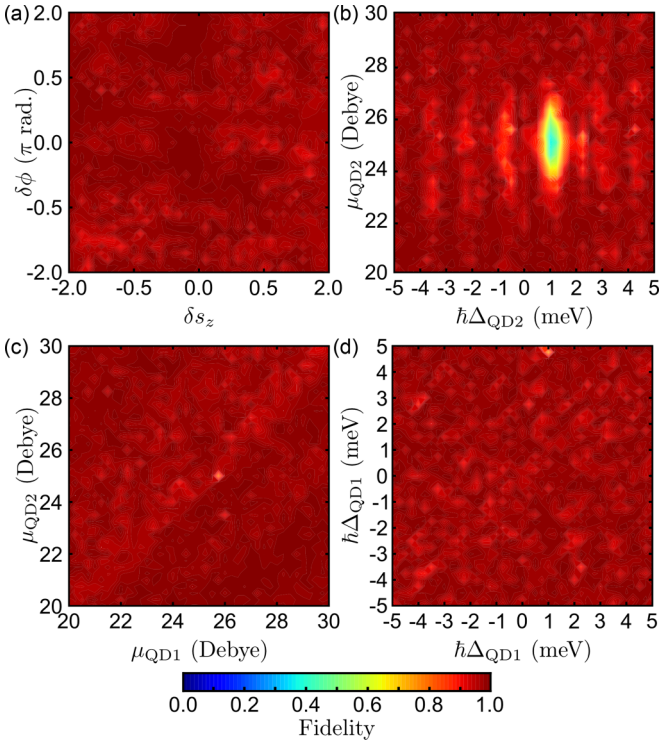

FIG. 2. (Color online) (a) Optimized fidelity as a function of the difference in phase and inversion of the two qubits for the optoelectronic properties used in Fig. 1. (b)–(d) Optimized fidelity of the quantum control process shown in Fig. 1 as a function of (b) the detuning of QD2 from the laser frequency [$\hbar\Delta_{QD2} = \hbar(\omega_{QD2} - \omega_l)$] and its dipole moment, while holding the properties of QD1 constant ($\hbar\omega_{QD1} = 1.00125$ eV and $\mu_{QD1} = 25$ debye), (c) the dipole moment of the two quantum dots while holding the transition frequencies constant ($\hbar\omega_{QD1} = 1.00125$ eV and $\hbar\omega_{QD1} = 0.99875$ eV), and (d) the detuning of the QD transitions from the laser frequency while holding the dipole moments constant ($\mu_{QD1} = 25$ debye and $\mu_{QD2} = 28$ debye).

and QD2 coincide. Nevertheless, for QDs with sufficiently different properties, optimized pulses can be engineered to implement the parallel single qubit rotation with high fidelity. In particular, it is not necessary to have a difference in both the dipole moment and transition energy for the two QDs: a difference in *either* property will suffice. This is evident from calculations that optimize the same control process as in Fig. 1 as a function of the dipole moments while holding the transition frequencies constant [Fig. 2(c)], and as a function of the transition frequencies while holding the dipole moments constant [Fig. 2(d)]. In all cases, we find that control pulse shapes realizing high fidelity gates may be found within the accessible parameter space of the pulse shaping system.

C. Parallel quantum control: Scaling the approach

The optimization scheme described here may be extended to independent simultaneous control of excitons in more than two quantum dots. The results in Fig. 2(b) show that independently addressing distinct QDs is possible provided that their optoelectronic properties are sufficiently different. Since a difference in either the dipole moment or the transition

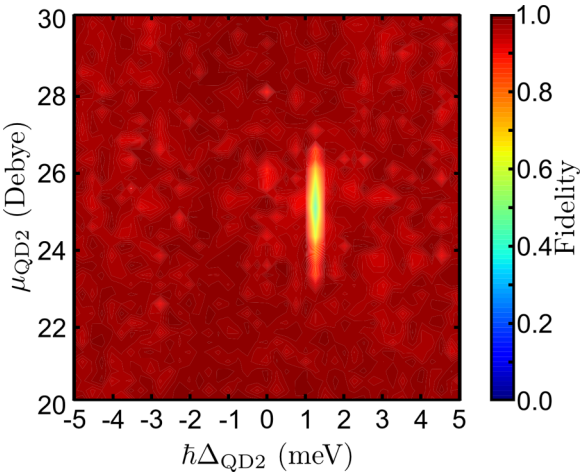

FIG. 3. (Color online) Same calculation as in Fig. 2(b) taking the assumption of a higher resolution pulse shaping system, incorporating a 640 pixel SLM.

energy is sufficient for high-fidelity control, we will focus here on differences in the transition energy of the two QDs. The width of the dip in fidelity in Fig. 2(b) versus transition energy is limited by the resolution of the SLM, which was assumed to contain 128 pixels. The calculation of Fig. 2(b) was repeated assuming a higher-resolution pulse shaping system incorporating a 640 pixel SLM. The results of these calculations are shown in Fig. 3. A larger SLM resolution expands the available parameter space for α and γ in Eq. (7) while keeping the maximum phase change per pixel constant. In Fig. 3, the width of the low-fidelity feature is below the resolution of the calculation mesh (0.25 meV), providing an upper bound on the minimum distinguishability in the transition energy required for independent high fidelity control of the two QDs. The fundamental limit on the number of QDs that could be controlled simultaneously will be determined by the resolution of the pulse shaping system. (For example, for the pulse bandwidth considered here, this resolution corresponds to 0.05 meV/pixel.)

For typical self-assembled QD ensembles, the transition energy spread is in the range 30 to 70 meV depending on the growth conditions and type of barrier material [40,43]. Using the upper bound value of 0.25 meV for the minimum difference in transition energy, this indicates that simultaneous high fidelity control of many QDs would be possible. The use of a more sophisticated phase mask function rather than the simple sinusoidal mask used here, as well as the freedom to employ combined amplitude and phase control, would aid in optimizing the performance of parallel quantum control of multiple quantum dots. One simple approach would be to utilize a phase-only mask parameterized by a superposition of several sinusoidal functions with independently adjustable parameters, which would permit sensitive control of various orders of spectral chirp at each of several QD resonances [37]. This approach exploits the ease of experimentally realizing arbitrary pulse shape control using standard, user-friendly pulse shaping systems while transferring the complexity to the design of the pulse shape in a physical system of QDs, for which modeling the quantum state dynamics is

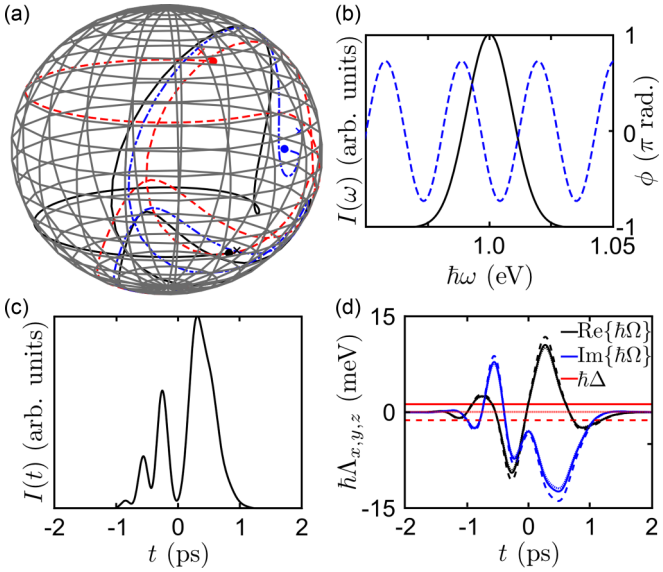

FIG. 4. (Color online) Application of OQC to the simultaneous manipulation of excitons in three QDs. For this calculation, the final state of the third quantum dot, QD3, with $\hbar\omega_{\mathrm{QD3}} = 1.00005$ eV and $\mu_{\mathrm{QD3}} = 24$ debye, is $|\psi_{\mathrm{QD3}}\rangle_{\mathrm{f}} = (|0\rangle + e^{-i3\pi/4}|1\rangle)/\sqrt{2}$, while for QD1 and QD2 the final states are given by Eqn. (8). (a) Bloch sphere dynamics for QD1, QD2, and QD3 are indicated by the black solid curve, the red dashed curve, and the blue dot-dashed curve, respectively. The optimal pulse in this case is defined by $q_{\mathrm{opt}} = (0.730\pi, 134\ \mathrm{fs}, -0.726\pi, 2.12\pi)$ and when implemented results in a quantum gate fidelity of 0.985. (b) The spectral amplitude (phase) of the pulse is indicated by a black solid (blue dashed) curve. (c) Temporal intensity of the shaped pulse. (d) The x, y, and z components of $\mathbf{\Lambda}$ are indicated by black, blue, and red curves, respectively, with solid curves corresponding to QD1, dashed curves corresponding to QD2, and dot-dashed curves corresponding to QD3.

straightforward. Numerically optimized quantum control involving three QDs is shown in Fig. 4 using the same single-cosine phase mask as for the two-dot control calculations considered here, illustrating the flexibility of the OQC approach as the number of QDs is increased. Our findings indicate that the simultaneous control of more than 10 QDs should be readily achievable in experimental implementations.

If combined with controllable entanglement between distant quantum dots via microcavity modes [50], this approach may enable the realization of complex instruction set quantum computing in a solid state system of QDs. In such a system, the laser pulse could be designed taking into account the differing resonance conditions for each QD in relation to the modes of the optical microcavity as well as the ability to tailor the energy and bandwidth of microcavity modes for optimized coupling of several QDs [51]. Such an achievement would complement recent experimental progress towards an integrated quantum dot nanophotonic chip [52–57], and would build upon the recent demonstration of a multiple-input AND gate using six qubits encoded in the rovibrational eigenstates of a lithium molecule [14]. In that demonstration, the laser pulse and final state read-out conditions were tailored to the individual resonances and strength of the coupling between the different rovibrational states. One could foresee engineering the QD ensemble size distribution to have a spread of transition energies that matches the bandwidth of convenient commercial laser systems, in line with successful efforts to obtain narrow energy distributions coinciding with telecommunications wavelengths for QD laser applications [43].

D. Tolerance to experimental uncertainties

In the presence of uncertainties in experimental parameters, the fidelity of the control process will be reduced. The primary limitation on the sensitivity of the fidelity to such non-ideal conditions is the choice here to impose a fixed read time [3 ps after $t = 0$ in Eq. (1)] due to the rapid evolution of the phase of the exciton qubit in any particular QD outside the pulse envelope. For instance, a laser tuning error of 0.05 nm produces a drop in fidelity of 0.01 averaged over the parameter space in Fig. 2(a). For comparison, the fidelity is much less sensitive to deviations in laser intensity: A typical specification for mode-locked laser systems of 0.5% gives a fidelity drop of only 0.001. In the implementation of circuit-model quantum computing with multiple control pulses, one could minimize such errors experimentally by incorporating active feedback on the relative time delays for different control pulses. Small deviations in qubit phase could also be compensated for by implementing empirical feedback to the pulse shaping system, so that the optimum mask parameters may be adjusted via a genetic algorithm. Such an approach would also benefit complex instruction set implementations. Quantum state read-out via differential transmission [58] or photocurrent [16] is only sensitive to the state occupations and so phase uncertainty would have no impact on the final quantum state detection. We also note that, while biexciton dynamics are not included in the present calculations, in full simulations of the coupled exciton-biexciton system it is possible to build into the OQC optimization the need to have the occupation of the biexciton state vanish at the end of the control pulse, as shown for the case of the C-ROT gate in Ref. [38].

E. Influence of dephasing

It is instructive to examine the influence of sources of dephasing of the exciton qubit on the fidelity of the quantum control process. Calculations within the relaxation time approximation incorporating typical measured dephasing and recombination times in InAs self-assembled QDs [59] indicate only a minor reduction in fidelity (e.g., a drop from 0.996 to 0.991 for the test gate in Fig. 1), reflecting the short time scale of the optical pulse relative to these decay times. We also examine the effects of a power-dependent dephasing process, often referred to as *excitation-induced* dephasing (EID), in which deformation potential coupling with longitudinal acoustic phonons causes transitions between the dressed states of the optically driven quantum dot system [48,60–63]. Such a process leads to damping of Rabi oscillations [48,61] and a dependence of the exciton inversion on the sign of pulse chirp in adiabatic rapid passage experiments [64,65]. The strength of the EID process is dictated by the real part of the exciton-phonon response function, $K(\omega)$, which is evaluated at the instantaneous value of $|\mathbf{\Lambda}|$. Taking a linear dispersion relation for the bulk phonon modes of the barrier

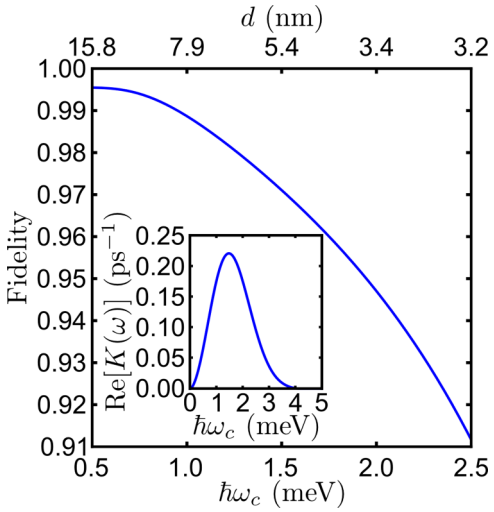

FIG. 5. (Color online) Fidelity for the calculation shown in Fig. 1 incorporating excitation-induced dephasing caused by coupling to longitudinal acoustic phonons as a function of the cutoff energy, $\hbar\omega_c$, of the exciton-phonon response. The phonon modes of bulk GaAs are assumed, for which $\alpha = 0.027$ ps^2. The top x axis shows the corresponding width of the norm squared of the carrier wave function. Inset: The calculated phonon response function taking $\hbar\omega_c = 1.38$ meV, corresponding to $d = 5.76$ nm.

material (chosen here as GaAs, appropriate for InAs/GaAs self-assembled quantum dots), and assuming a spherical quantum dot for simplicity with a carrier wave function of the form $\psi(x) \propto \exp[-2\ln(2)x^2/d^2]$, the exciton-phonon response function is given by [62]

$$\mathrm{Re}[K(\omega)] = \frac{\pi}{2}\alpha\omega^3 e^{-\omega^2/\omega_c^2}\coth(\omega/2k_BT), \qquad (9)$$

where α is a coupling constant that depends on the deformation-potential constants of the barrier material, T is the temperature, and k_B is the Boltzmann constant. The exciton-phonon response function is characterized by a cutoff frequency, ω_c, that is inversely proportional to the spatial extent of the wave function, d [60]. This implies that the impact of EID on the fidelity of the quantum control process depends on both the size of the quantum dot and the magnitude of the instantaneous Rabi energy. Figure 5 shows the fidelity for the calculation shown in Fig. 1 as a function of $\hbar\omega_c$ and d for $T = 10$ K. For cutoff energies less than $\sim$1.38 meV ($d > 5.76$ nm), the reduction in fidelity is less than 2 %. This error is quite modest, but nevertheless would be reduced by incorporating EID into the OQC numerical optimization due to the dependence of this process on the pulse shape. In addition, the exploration of alternate mask parametrizations may be beneficial. The use of engineered quantum dot distributions with a larger mean size would also reduce the influence of EID and increase the fidelity of quantum control.

IV. CONCLUSIONS

In conclusion, we have applied optimal quantum control in numerical simulations of laser-driven dynamics of excitons in semiconductor quantum dots. Our findings demonstrate the feasibility of independent, simultaneous SU(2) control of qubits in two or more quantum dots using a single shaped laser pulse. Our results show that pulse engineering with a simple sinusoidal phase mask leads to high-fidelity parallel single qubit rotations over a wide range of optoelectronic properties and final states, indicating that this is a versatile approach to multiqubit control. Quantum control processes optimized using this scheme could either be implemented directly in experiments, as demonstrated in Ref. [37], or provide seeding candidates for the initial population of a genetic feedback algorithm, which would aid in the compensation for experimental uncertainties. The use of arbitrary pulse shaping of broad-bandwidth control pulses builds upon the recent experimental demonstration of simultaneous $(\pi, 2\pi)$ rotations [37] and a subpicosecond adiabatic rapid passage gate [64]. The results presented here enhance the potential scalability of QD-based platforms for quantum information applications.

ACKNOWLEDGMENTS

The authors thank the Natural Sciences and Engineering Council of Canada, Lockheed Martin Corporation, and the Canada Research Chairs program for financial support.

[1] A. P. Peirce, M. A. Dahleh, and H. Rabitz, Optimal control of quantum-mechanical systems: Existence, numerical approximation, and applications, Phys. Rev. A **37**, 4950 (1988).
[2] R. Kosloff, S. Rice, P. Gaspard, S. Tersigni, and D. Tannor, Wavepacket dancing: Achieving chemical selectivity by shaping light pulses, Chem. Phys. **139**, 201 (1989).
[3] J. Werschnik and E. K. U. Gross, Quantum optimal control theory, J. Phys. B **40**, R175 (2007).
[4] D. J. Egger and F. K. Wilhelm, Adaptive Hybrid Optimal Quantum Control for Imprecisely Characterized Systems, Phys. Rev. Lett. **112**, 240503 (2014).
[5] J. Kelly *et al.*, Optimal Quantum Control Using Randomized Benchmarking, Phys. Rev. Lett. **112**, 240504 (2014).
[6] R. J. Levis, G. M. Menkir, and H. Rabitz, Selective Bond Dissociation and Rearrangement with Optimally Tailored, Strong-Field Laser Pulses, Science **292**, 709 (2001).
[7] A. Assion, T. Baumert, M. Bergt, T. Brixner, B. Kiefer, V. Seyfried, M. Strehle, and G. Gerber, Control of chemical reactions by feedback-optimized phase-shaped femtosecond laser pulses, Science **282**, 919 (1998).
[8] D. Pestov *et al.*, Optimizing the laser-pulse configuration for coherent Raman spectroscopy, Science **316**, 265 (2007).
[9] R. Bartels, S. Backus, E. Zeek, L. Misoguti, G. Vdovin, I. P. Christov, M. M. Murnane, and H. C. Kapteyn, Shaped-pulse optimization of coherent emission of high-harmonic soft X-rays, Nature (London) **406**, 164 (2000).
[10] T. Rickes, J. P. Marangos, and T. Halfmann, Enhancement of third-harmonic generation by Stark-chirped rapid adiabatic passage, Opt. Commun. **227**, 133 (2003).
[11] T. Choi, S. Debnath, T. A. Manning, C. Figgatt, Z.-X. Gong, L.-M. Duan, and C. Monroe, Optimal Quantum Control of Multimode Couplings between Trapped Ion Qubits

for Scalable Entanglement, Phys. Rev. Lett. **112**, 190502 (2014).
[12] F. Dolde *et al.*, High-fidelity spin entanglement using optimal control, Nat. Commun. **5**, 3371 (2014).
[13] G. D. Sanders, K. W. Kim, and W. C. Holton, Quantum computing with complex instruction sets, Phys. Rev. A **59**, 1098 (1999).
[14] Z. Amitay, R. Kosloff, and S. R. Leone, Experimental coherent computation of a multiple-input AND gate using pure molecular superpositions, Chem. Phys. Lett. **359**, 8 (2002).
[15] T. H. Stievater, X. Li, D. G. Steel, D. Gammon, D. S. Katzer, D. Park, C. Piermarocchi, and L. J. Sham, Rabi Oscillations of Excitons in Single Quantum Dots, Phys. Rev. Lett. **87**, 133603 (2001).
[16] A. Zrenner, E. Beham, S. Stufler, F. Findeis, M. Bichler, and G. Abstreiter, Coherent properties of a two-level system based on a quantum-dot photodiode, Nature (London) **418**, 612 (2002).
[17] H. Kamada, H. Gotoh, J. Temmyo, T. Takagahara, and H. Ando, Exciton Rabi Oscillation in a Single Quantum Dot, Phys. Rev. Lett. **87**, 246401 (2001).
[18] H. Htoon, T. Takagahara, D. Kulik, O. Baklenov, A. L. Holmes, and C. K. Shih, Interplay of Rabi Oscillations and Quantum Interference in Semiconductor Quantum Dots, Phys. Rev. Lett. **88**, 087401 (2002).
[19] P. Borri, W. Langbein, S. Schneider, U. Woggon, R. L. Sellin, D. Ouyang, and D. Bimberg, Rabi oscillations in the excitonic ground-state transition of InGaAs quantum dots, Phys. Rev. B **66**, 081306(R) (2002).
[20] T. Flissikowski, A. Betke, I. A. Akimov, and F. Henneberger, Two-Photon Coherent Control of a Single Quantum Dot, Phys. Rev. Lett. **92**, 227401 (2004).
[21] S. Stufler, P. Machnikowski, P. Ester, M. Bichler, V. M. Axt, T. Kuhn, and A. Zrenner, Two-photon Rabi oscillations in a single $In_xGa_{1-x}As/GaAs$ quantum dot, Phys. Rev. B **73**, 125304 (2006).
[22] D. Press, T. D. Ladd, B. Zhang, and Y. Yamamoto, Complete quantum control of a single quantum dot spin using ultrafast optical pulses, Nature (London) **456**, 218 (2008).
[23] B. D. Gerardot, D. Brunner, P. A. Dalgarno, P. Öhberg, S Seidl, M. Kroner, K. Karrai, N. G. Stoltz, P. M. Petroff, and R. J. Warburton, Optical pumping of a single hole spin in a quantum dot, Nature (London) **451**, 441 (2008).
[24] N. H. Bonadeo, J. Erland, D. Gammon, D. Park, D. S. Katzer, and D. G. Steel, Coherent optical control of the quantum state of a single quantum dot, Science **282**, 1473 (1998).
[25] L. Besombes, J. J. Baumberg, and J. Motohisa, Coherent Spectroscopy of Optically Gated Charged Single InGaAs Quantum Dots, Phys. Rev. Lett. **90**, 257402 (2003).
[26] S. Stufler, P. Ester, A. Zrenner, and M. Bichler, Quantum optical properties of a single $In_xGa_{1-x}As$-GaAs quantum dot two-level system, Phys. Rev. B **72**, 121301(R) (2005).
[27] Y. Wu, X. Li, L. M. Duan, D. G. Steel, and D. Gammon, Density Matrix Tomography through Sequential Coherent Optical Rotations of an Exciton Qubit in a Single Quantum Dot, Phys. Rev. Lett. **96**, 087402 (2006).
[28] R. S. Kolodka, A. J. Ramsay, J. Skiba-Szymanska, P. W. Fry, H. Y. Liu, A. M. Fox, and M. S. Skolnick, Inversion recovery of single quantum-dot exciton based qubit, Phys. Rev. B **75**, 193306 (2007).
[29] K. Müller, T. Kaldewey, R. Ripszam, J. S. Wildmann, A. Bechtold, M. Bichler, G. Koblmüller, G. Abstreiter, and J. J. Finley, All optical quantum control of a spin-quantum state and ultrafast transduction into an electric current, Sci. Rep. **3**, 1906 (2013).
[30] E. Poem, O. Kenneth, Y. Kodriano, Y. Benny, S. Khatsevich, J. E. Avron, and D. Gershoni, Optically Induced Rotation of an Exciton Spin in a Semiconductor Quantum Dot, Phys. Rev. Lett. **107**, 087401 (2011).
[31] Y. Kodriano, I. Schwartz, E. Poem, Y. Benny, R. Presman, T. A. Truong, P. M. Petroff, and D. Gershoni, Complete control of a matter qubit using a single picosecond laser pulse, Phys. Rev. B **85**, 241304(R) (2012).
[32] X. Li, Y. Wu, D. Steel, D. Gammon, T. H. Stievater, D. S. Katzer, D. Park, C. Piermarocchi, and L. J. Sham, An all-optical quantum gate in a semiconductor quantum dot, Science **301**, 809 (2003).
[33] S. J. Boyle, A. J. Ramsay, F. Bello, H. Y. Liu, M. Hopkinson, A. M. Fox, and M. S. Skolnick, Two-qubit conditional quantum-logic operation in a single self-assembled quantum dot, Phys. Rev. B **78**, 075301 (2008).
[34] G. Chen, N. H. Bonadeo, D. G. Steel, D. Gammon, D. S. Katzer, D. Park, and L. J. Sham, Optically induced entanglement of excitons in a single quantum dot, Science **289**, 1906 (2000).
[35] A. Gamouras, M. Britton, M. M. Khairy, R. Mathew, D. Dalacu, P. Poole, D. Poitras, R. L. Williams, and K. C. Hall, Energy-selective optical excitation and detection in InAs/InP quantum dot ensembles using a one-dimensional optical microcavity, Appl. Phys. Lett. **103**, 253109 (2013).
[36] A. Gamouras, R. Mathew, and K. C. Hall, Optically engineered ultrafast pulses for controlled rotations of exciton qubits in semiconductor quantum dots, J. Appl. Phys. **112**, 014313 (2012).
[37] A. Gamouras, R. Mathew, S. Freisem, D. G. Deppe, and K. C. Hall, Simultaneous deterministic control of distant qubits in two semiconductor quantum dots, Nano Lett. **13**, 4666 (2013).
[38] R. Mathew, C. E. Pryor, M. E. Flatté, and K. C. Hall, Optimal quantum control for conditional rotation of exciton qubits in semiconductor quantum dots, Phys. Rev. B **84**, 205322 (2011).
[39] F. Troiani, U. Hohenester, and E. Molinari, Exploiting exciton-exciton interactions in semiconductor quantum dots for quantum-information processing, Phys. Rev. B **62**, R2263 (2000).
[40] A. J. Ramsay, A review of the coherent optical control of the exciton and spin states of semiconductor quantum dots, Semicond. Sci. Technol. **25**, 103001 (2010).
[41] H. Y. Liu *et al.*, Improved performance of 1.3 μm multilayer InAs quantum-dot lasers using a high-growth-temperature GaAs spacer layer, Appl. Phys. Lett. **85**, 704 (2004).
[42] Y. C. Zhang, A. Pancholi, and V. G. Stoleru, Size-dependent radiative lifetime in vertically stacked (In,Ga)As quantum dot structures, Appl. Phys. Lett. **90**, 183104 (2007).
[43] D. Huffaker, G. Park, Z. Zou, O. Shchekin, and D. Deppe, Continuous-wave low-threshold performance of 1.3-μm InGaAs-GaAs quantum-dot lasers, IEEE J. Select. Topics Quantum Electron. **6**, 452 (2000).
[44] D. Gammon, E. S. Snow, B. V. Shanabrook, D. S. Katzer, and D. Park, Homogeneous linewidths in the optical spectrum of a single gallium arsenide quantum dot, Science **273**, 87 (1996).
[45] A. Muller, Q. Q. Wang, P. Bianucci, C. K. Shih, and Q. K. Xue, Determination of anisotropic dipole moments in self-assembled

quantum dots using Rabi oscillations, Appl. Phys. Lett. **84**, 981 (2004).

[46] Q. Q. Wang, A. Muller, M. T. Cheng, H. J. Zhou, P. Bianucci, and C. K. Shih, Coherent Control of a V-Type Three-Level System in a Single Quantum Dot, Phys. Rev. Lett. **95**, 187404 (2005).

[47] A. M. Weiner, Femtosecond pulse shaping using spatial light modulators, Rev. Sci. Instrum. **71**, 1929 (2000).

[48] A. J. Ramsay, T. M. Godden, S. J. Boyle, E. M. Gauger, A. Nazir, B. W. Lovett, A. M. Fox, and M. S. Skolnick, Phonon-Induced Rabi-Frequency Renormalization of Optically Driven Single InGaAs/GaAs Quantum Dots, Phys. Rev. Lett. **105**, 177402 (2010).

[49] I. M. Sobol', Distribution of points in a cube and approximate evaluation of integrals, USSR J. Comput. Math. Math. Phys. **7**, 86 (1967).

[50] A. Imamoglu, D. D. Awschalom, G. Burkard, D. P. DiVincenzo, D. Loss, M. Sherwin, and A. Small, Quantum Information Processing Using Quantum Dot Spins and Cavity QED, Phys. Rev. Lett. **83**, 4204 (1999).

[51] K. Hennessy, A. Badolato, M. Winger, D. Gerace, M. Atatüre, S. Gulde, S. Fält, E. L. Hu, and A. Imamoglu, Quantum nature of a strongly coupled single quantum dot cavity system, Nature (London) **445**, 896 (2007).

[52] K. De Greve *et al.*, Quantum-dot spin–photon entanglement via frequency downconversion to telecom wavelength, Nature (London) **491**, 421 (2012).

[53] W. B. Gao, P. Fallahi, E. Togan, J. Miguel-Sanchez, and A. Imamoglu, Observation of entanglement between a quantum dot spin and a single photon, Nature (London) **491**, 426 (2012).

[54] W. B. Gao, P. Fallahi, E. Togan, A. Delteil, Y. S. Chin, J. Miguel-Sanchez, and A. Imamoğlu, Quantum teleportation from a propagating photon to a solid state spin qubit, Nat. Commun. **4**, 2744 (2013).

[55] J. L. O'Brien, A. Furusawa, and J. Vuckovic, Photonic quantum technologies, Nat. Photon. **3**, 687 (2009).

[56] M. N. Makhonin, J. E. Dixon, R. J. Coles, B. Royall, I. J. Luxmoore, E. Clarke, M. Hugues, M. S. Skolnick, and A. Mark Fox, Waveguide coupled resonance fluorescence from on-chip quantum emitter, Nano Lett. **14**, 6997 (2014).

[57] M. Mikulics and H. Hardtdegen, Nano-LED array fabrication suitable for future single photon lithography, Nanotechnology **26**, 185302 (2015).

[58] E. D. Kim, K. Truex, Y. Wu, A. Amo, X. Xu, D. G. Steel, A. S. Bracker, D. Gammon, and L. J. Sham, Picosecond optical spectroscopy of a single negatively charged self-assembled InAs quantum dot, Appl. Phys. Lett. **97**, 113110 (2010).

[59] P. Borri, W. Langbein, S. Schneider, U. Woggon, R. L. Sellin, D. Ouyang, and D. Bimberg, Ultralong Dephasing Time in InGaAs Quantum Dots, Phys. Rev. Lett. **87**, 157401 (2001).

[60] A. Nazir, Photon statistics from a resonantly driven quantum dot, Phys. Rev. B **78**, 153309 (2008).

[61] A. J. Ramsay, A. V. Gopal, E. M. Gauger, A. Nazir, B. W. Lovett, A. M. Fox, and M. S. Skolnick, Damping of Exciton Rabi Rotations by Acoustic Phonons in Optically Excited InGaAs/GaAs Quantum Dots, Phys. Rev. Lett. **104**, 017402 (2010).

[62] A. J. Ramsay, T. M. Godden, S. J. Boyle, E. M. Gauger, A. Nazir, B. W. Lovett, A. V. Gopal, A. M. Fox, and M. S. Skolnick, Effect of detuning on the phonon induced dephasing of optically driven InGaAs/GaAs quantum dots, J. Appl. Phys. **109**, 102415 (2011).

[63] A. Debnath, C. Meier, B. Chatel, and T. Amand, Chirped laser excitation of quantum dot excitons coupled to a phonon bath, Phys. Rev. B **86**, 161304(R) (2012).

[64] R. Mathew, E. Dilcher, A. Gamouras, A. Ramachandran, H. Y. S. Yang, S. Freisem, D. Deppe, and K. C. Hall, Subpicosecond adiabatic rapid passage on a single semiconductor quantum dot: Phonon-mediated dephasing in the strong-driving regime, Phys. Rev. B **90**, 035316 (2014).

[65] Y.-J. Wei, Y.-M. He, M.-C. Chen, Y.-N. Hu, Y. He, D. Wu, C. Schneider, M. Kamp, S. Hofling, C.-Y. Lu, and J.-W. Pan, Deterministic and robust generation of single photons from a single quantum dot with 99.5% indistinguishability using adiabatic rapid passage, Nano Lett. **14**, 6515 (2014).